# SPATIAL FOCUSING AND INTERFERENCE REDUCTION USING MISO TIME REVERSAL IN AN INDOOR APPLICATION

*Xin Zhou, Patrick Claus Friedrich Eggers, Persefoni Kyritsi,*
*Jørgen Bach Andersen, Gert Frølund Pedersen, Jesper Ødum Nilsen*

Antennas, Propagation and Radio Networking Section,
Department of Electronic Systems,
Aalborg University, Denmark
(*xz, pe, persa, jba, gfp, jni*@es.aau.dk)

## ABSTRACT

This paper evaluates the spatial focusing performance of the Time Reversal (TR) method in a multiple input single output (MISO) situation with experimental data. For the target user, the received signal is related to the channel link from the transmitter to the target receiver. The received power increases as we enlarge the array size, and it increases by *15.6*dB with *16* transmit antennas, compared to the single link. For the eavesdropper, the received signal is determined by both the channel link from the transmitter to the target user and the channel link from the transmitter to the eavesdropper. In terms of unbalanced branch power, the minimum average Eavesdropping Margin (*EM*) and Peak Eavesdropping Margin ($EM_{\text{Peak}}$) are *14*dB and *13*dB from *16* transmit elements.

***Index Terms***— MISO, time reversal, spatial focusing

## 1. INTRODUCTION

Time Reversal (TR) is a pre-filtering scheme, which has the potential to achieve time compression and spatial focusing [1]-[6]. The time compression refers to the capability of reducing the effective length of the resulting impulse response (IR) in the time domain, and the spatial focusing indicates the beamforming capability by concentrating the signal on the target user. Furthermore, the application of the TR method can achieve transmit diversity and has the potential to tolerate a rather simple receiver.

The concept of TR was introduced in acoustic wave applications [1]-[3], and has recently been studied in the field of wireless communications by using electromagnetic waves [4]-[8], specifically in the multiple input single output (MISO) setting. So far, measurement investigations of MISO TR have been focused on either the time compression property [6]-[7], or the spatial focusing performance in outdoor environments [7]-[8]. In this paper, we concentrate on the spatial focusing performance of TR in a Wideband (WB) indoor environment with quasi-static channel conditions.

The prerequisite for the application of TR is that the transmitter (Tx) has the Channel State Information (CSI). This can be achieved either from the Uplink transmission where by the Tx acquires the CSI, or through a feedback loop where the receiver (Rx) estimates the CSI and feeds it back to the Tx [6], [9]. In this paper, we assume perfect channel estimation and synchronization, and we only consider a MISO Downlink situation.

In the following, bold symbols denote matrices and underlined symbols indicate vectors. $(\cdot)^*$ and $(\cdot)^H$ are the complex conjugate and the hermitian of the argument $(\cdot)$, respectively. $E[\cdot]$ is the expected value of the argument $[\cdot]$. The superscripts 'Target' and 'Eav' are the notations of the target user and the eavesdropper, respectively.

## 2. MISO TIME REVERSAL

Let us assume a MISO communication system with *M* transmit antennas and *1* receive antenna. The transmitted and received data streams are denoted as *x(t)* and *y(t)*, respectively. The channel IR from the *m*-th Tx antenna to the

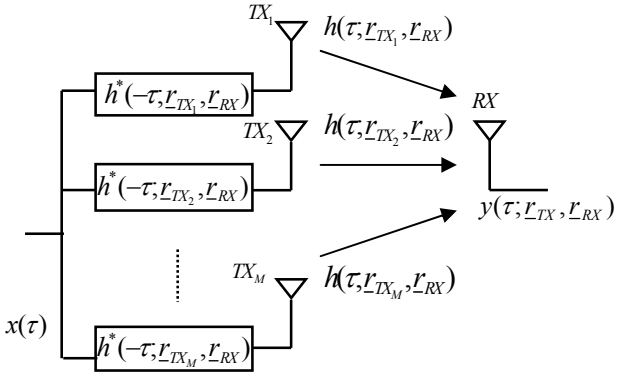


Figure 1. MISO Time Reversal Diagram.

Rx is expressed as $h_m$, where $h_m = h(\tau; \underline{r}_{TX_m}, \underline{r}_{RX})$. $\tau$ and $r$ are the delay and space variables, respectively. $\underline{r}_{TXm}$ denotes the location of the $m$-th Tx antenna, and $\underline{r}_{RX}$ indicates the position of the Rx. We apply the TR scheme, by adding filters at the Tx side, where the filter at the $m$-th Tx element is the complex-conjugate time-reversed channel IR from the $m$-th Tx antenna to the target Rx (see Figure 1).

In the evaluation of the spatial focusing performance, we distinguish 2 different receivers: the target user and the eavesdropper. In the absence of noise, the received signal at the target user ( $y(\tau; \underline{r}_{TX}, \underline{r}_{RX}^{\text{Target}})$ ) and the eavesdropper ( $y(\tau; \underline{r}_{TX}, \underline{r}_{RX}^{\text{Eav}})$ ) can be expressed as:

$$y(\tau; \underline{r}_{TX}, \underline{r}_{RX}^{\text{Target}}) = \alpha \cdot \sum_{m=1}^{M} x(\tau) \otimes h^*(-\tau; \underline{r}_{TX_m}, \underline{r}_{RX}^{\text{Target}}) \otimes h(\tau; \underline{r}_{TX_m}, \underline{r}_{RX}^{\text{Target}})$$
$$= \alpha \cdot x(\tau) \otimes \sum_{m=1}^{M} R^{\text{auto}}(\tau; \underline{r}_{TX_m}, \underline{r}_{RX}^{\text{Target}}) \quad (1)$$

$$y(\tau; \underline{r}_{TX}, \underline{r}_{RX}^{\text{Eav}}) = \alpha \cdot \sum_{m=1}^{M} x(\tau) \otimes h^*(-\tau; \underline{r}_{TX_m}, \underline{r}_{RX}^{\text{Target}}) \otimes h(\tau; \underline{r}_{TX_m}, \underline{r}_{RX}^{\text{Eav}}) \quad (2)$$

$\underline{r}_{RX}^{\text{Target}}$ and $\underline{r}_{RX}^{\text{Eav}}$ are the locations of Rx from the target user and eavesdropper, respectively. $R^{\text{auto}}(\cdot)$ indicates the auto-correlation function. $\alpha$ is a normalization factor so that the transmitted power is 1, namely

$$\alpha = \frac{1}{\sqrt{\sum_{m=1}^{M} \int_{\tau=0}^{\tau_{\max}} \left| h^*(-\tau; \underline{r}_{TX_m}, \underline{r}_{RX}^{\text{Target}}) \right|^2 d\tau}} \quad (3)$$

where $\tau_{max}$ denotes the maximum delay of the channel IR.

We define the 'effective channel IR' for both the target user ( $h_{\text{eff}}^{\text{Target}}$ ) and the eavesdroppers ( $h_{\text{eff}}^{\text{Eav}}$ ) as:

$$h_{\text{eff}}^{\text{Target}}(\tau; \underline{r}_{TX}, \underline{r}_{RX}^{\text{Target}}) = \alpha \cdot \sum_{m=1}^{M} R^{\text{auto}}(\tau; \underline{r}_{TX_m}, \underline{r}_{RX}^{\text{Target}}) \quad (4)$$

$$h_{\text{eff}}^{\text{Eav}}(\tau; \underline{r}_{TX}, \underline{r}_{RX}^{\text{Target}}) = \alpha \cdot \sum_{m=1}^{M} h^*(-\tau; \underline{r}_{TX_m}, \underline{r}_{RX}^{\text{Target}}) \otimes h(\tau; \underline{r}_{TX_m}, \underline{r}_{RX}^{\text{Eav}}) \quad (5)$$

From equations (1) and (2), we can observe that the received signals at the target user and the eavesdropper are related to the auto- and cross-correlation functions of the channel IRs, respectively. Therefore, the difference of these resulting correlation functions attracts our interest in the spatial focusing performance.

With respect to the effective channel IR for the target user, we are interested in the received signal power at $\tau=0$ ($P^{\text{Target}}$), where the sidelobes of the effective channel IR are significantly compressed as the number of Tx antennas increases.

$$P^{\text{Target}} = | y(0; \underline{r}_{TX}, \underline{r}_{RX}^{\text{Target}}) |^2 \quad (6)$$

Regarding the effective channel IR for the eavesdropper, we evaluate both the power at the same time lag as the intended user ($P^{\text{Eav}}$), namely $\tau=0$, and the peak power over the delay domain ( $P_{\text{Peak}}^{\text{Eav}}$ ).

$$P^{\text{Eav}} = | y(0; \underline{r}_{TX}, \underline{r}_{RX}^{\text{Eav}}) |^2 \quad (7)$$

$$P_{\text{Peak}}^{\text{Eav}} = \max | y(\tau; \underline{r}_{TX}, \underline{r}_{RX}^{\text{Eav}}) |^2 \quad (8)$$

We further define the Eavesdropping Margin at $\tau=0$ ($EM$) and the Peak Eavesdropping Margin ($EM_{\text{Peak}}$) where we take the maximum power over delay domain for both the target and the eavesdropper:

$$EM = \frac{P^{\text{Target}}}{P^{\text{Eav}}} = \frac{| y(0; \underline{r}_{TX}, \underline{r}_{RX}^{\text{Target}}) |^2}{| y(0; \underline{r}_{TX}, \underline{r}_{RX}^{\text{Eav}}) |^2} \quad (9)$$

$$EM_{\text{Peak}} = \frac{P^{\text{Target}}}{P_{\text{Peak}}^{\text{Eav}}} = \frac{| y(0; \underline{r}_{TX}, \underline{r}_{RX}^{\text{Target}}) |^2}{\max(| y(\tau; \underline{r}_{TX}, \underline{r}_{RX}^{\text{Eav}}) |^2)}$$
$$= \frac{\max(| y(\tau; \underline{r}_{TX}, \underline{r}_{RX}^{\text{Target}}) |^2)}{\max(| y(\tau; \underline{r}_{TX}, \underline{r}_{RX}^{\text{Eav}}) |^2)} \quad (10)$$

## 3. MEASUREMENTS

In this indoor experiment, the carrier frequency was *5.8*GHz (wavelength $\lambda$=*5*cm). The instantaneous channel IR is obtained from *16* Tx antennas with a sampling rate of *60*Hz. The total period of the measurement is around *15*s, i.e. *900* samples. However, we only select *70* samples that behave in a relatively stationary manner. The measurements are taken in a building with several partitions made up by *1.5*m-height wooden boards (see Figure 2).

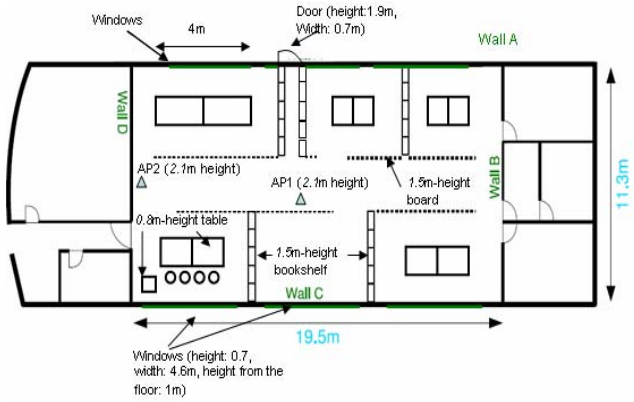


Figure 2. Measurement room layout: Tx arrays (AP1 and AP2), Rxs (*4* users sit around the table).

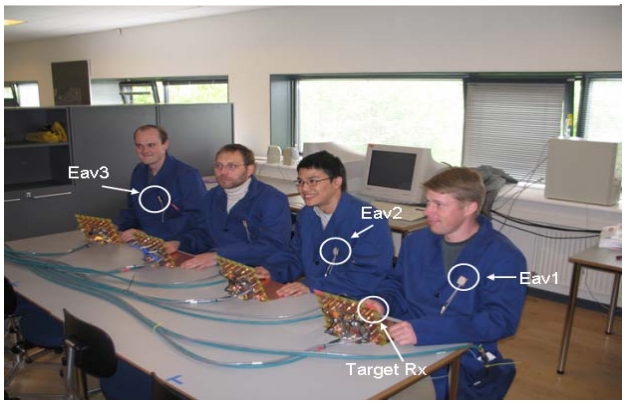


Figure 3. Photo of Rx arrangements: 4 users sit by the table, and 4 Rx antennas are used (Target Rx, Eav1, Eav2 and Eav3).

Two Access Points (APs) are arranged in a corridor at a height of *2.1*m, and each AP is mounted with *8* antenna elements. 4 users sit around the table (*0.8*m height) and face the APs. The outside walls of the building are made of bricks, and have glass windows. The window frame is made of aluminum. Each user has *2* types of Rx antennas: laptop and body mounted antennas, and there are *4* elements of each type on each user. During the measurements, each user mimics the behavior of typing at the laptop keyboard. In this measurement, we use *1* antenna on the laptop as the target user, and *3* body mounted antennas as the eavesdroppers, namely Eav1, Eav2 and Eav3 (see Figure 3).

## 4. SPATIAL FOCUSING PERFORMANCE

This section evaluates the spatial focusing performance of TR in a MISO situation, in terms of the received power and the average *EM*. In order to evaluate the influence of the difference among channel links, we rearrange the channel links from the Tx antennas to the intended Rx in an ascending order of their mean branch power, so that adding one more Tx antenna will always lead to involving a channel link with higher average power than the links which are currently used. In addition, the normalization factor $\alpha$ is re-calculated when we add one more transmit antenna, so that the total transmit power is *1*.

### 4.1. Average Signal Power

In this subsection, we look at the intended signal at both the target and the eavesdropper, by showing the average received signal power.

#### *4.1.1. Average Received Power at $\tau$=0*

We first investigate the average power of the received signal at $\tau$=*0* for the target user and the *3* eavesdroppers, with respect to different number of Tx antennas from the *2* APs (see Figure 4).

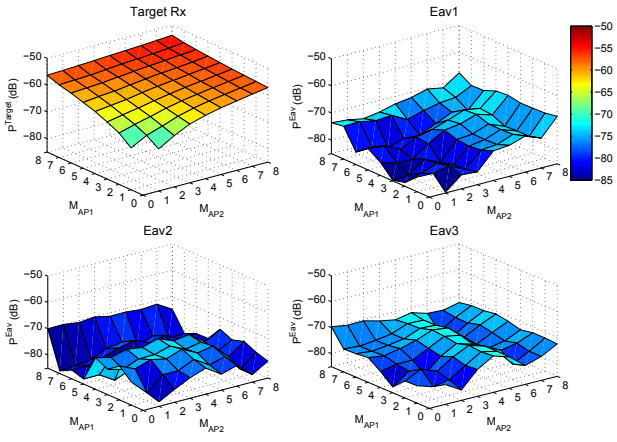


Figure 4. Average received signal power at $\tau$=*0* with respect to the number of Tx antennas at AP1 ($M_{AP1}$) and AP2 ($M_{AP2}$), respectively.

We expect the received signal power to increase by *6*dB for the target and *3*dB for the eavesdropper, per doubling of the number of Tx antennas. This can not be observed in Figure 4, due to the non-equal branch power both within each AP and between APs. However, we still can see the increasing trend of the peak power as the number of Tx antenna increases. For eavesdroppers, the received signals add incoherently at $\tau$=*0*, which leads to a rough surface. Compared to the single link (*1* Tx antenna from either AP1 and AP2 to *1* Rx antenna), the received signal power from *16* Tx antennas increases by *15.6*dB for the target user. For the eavesdropper, a minimum and a maximum increment of *1.4*dB and *17.2*dB are obtained from *16* transmit elements, respectively.

In Figure 5, we show the mean power as more transmit antennas are added as a function of the individual effective channel link in an ascending order. As we can see, the power of the effective channel IRs are unbalanced from *2* APs. The increase in received signal power as more antennas are used at transmitters, is determined by the power increment of the effective channel link. Due to the coherent addition for the peak power of the target user, the increase in peak power at the target user is directly proportional to the increment of the power of the individual effective channel.

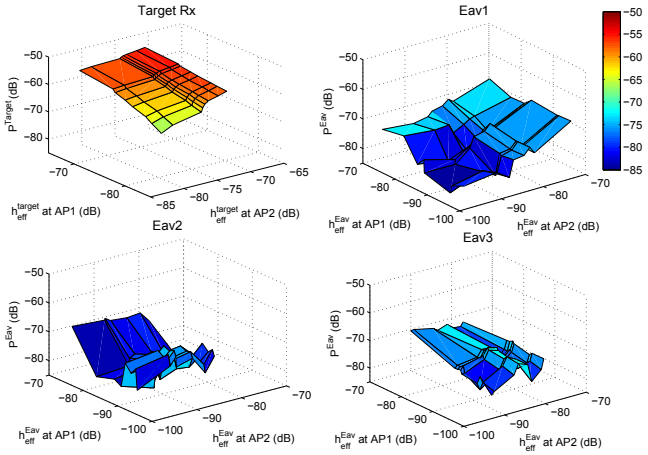


Figure 5. Average received signal power at $\tau$=*0* with respect to Mean power of individual effective channel link from AP1 and AP2, respectively.

In order to illustrate the variation of the power for the eavesdropper, we investigate the phase difference between the current effective channel and the summation of the previous channels, and its influence on the variation of the increasing/ decreasing trend of the received signal power. We investigate specifically the phase difference ($\theta_L$) between the effective channel IR after the summation of (*L-1*) terms and the cross-correlation of the *L*-th term at $\tau$=*0*. Each term

corresponds to the contribution from *1* Tx antenna at either AP1 and AP2.

$$\theta_L = \measuredangle\left[\sum_{m=1}^{L-1} \underline{h}_m^{\text{Eav}} \cdot (\underline{h}_m^{\text{Target}})^{\text{H}}\right] - \measuredangle\left[\underline{h}_L^{\text{Eav}} \cdot (\underline{h}_L^{\text{Target}})^{\text{H}}\right] \quad (11)$$

We show $cos(\text{E}[\theta_L])$ in Table 1. The value varies from *-1* to *1*, which indicates the trend of 2 vectors from completely non-coherent to coherent. For instance, $L=7$ for Eav1 from AP1, $cos(\text{E}[\theta_L])=1$. This means the *7*-th effective channel link is added coherently with the summation of the previous *6* links. Hence the received signal power increases at this point (See Figure 5, the right upper plot for Eav1). At $L=8$, $cos(\text{E}[\theta_L])=-0.8$, which indicates the non-coherent phase between the *8*-th effective channel IR and the summation of previous *7* effective channel IRs. Therefore, the received signal power does not increase, though we add one more antenna at the transmit side.

Table1. values of $cos(\text{E}[\theta_L])$ with respect to $L$ from *2* to *8*.

| Configuration | | $L$ | | | | | | |
|---|---|---|---|---|---|---|---|---|
| | | *2* | *3* | *4* | *5* | *6* | *7* | *8* |
| AP1 | Eav1 | *-0.5* | *-0.6* | *-0.6* | *-0.1* | *-0.7* | ***1.0*** | ***-0.8*** |
| | Eav2 | *0.2* | *-0.5* | *0.7* | *0.4* | *-0.6* | *-0.6* | *0.6* |
| | Eav3 | *-0.3* | *-0.7* | *-0.8* | *0.9* | *-0.5* | *0.3* | *-0.8* |
| AP2 | Eav1 | *-0.1* | *-0.1* | *0.2* | *0* | *0.4* | *-0.6* | *0.5* |
| | Eav2 | *-0.7* | *0.4* | *-0.1* | *-0.9* | *0.7* | *-0.6* | *0.3* |
| | Eav3 | *-0.6* | *0.8* | *0.9* | *-0.3* | *-0.8* | *-0.3* | *0.5* |

#### *4.1.2. Average Peak Power over Delay Domain*

We show the peak power over the delay domain for the target user and the eavesdropper in Figure 6. This value describes the maximum power the eavesdropper may intercept from the signal intended to the target over the delay domain. Therefore, this received signal power at the eavesdropper can be higher than the one observed at the same eavesdropper at $\tau=0$. This is the result shown in Figure 4. This maximum signal power at the eavesdropper is more robust to the addition of more Tx antennas, i.e. it fluctuates less, than the received power at at $\tau=0$. For the target, the signal power at the target is the same as the one shown in Figure 4, because the power at $\tau=0$ in the auto-correlation function is the maximum power. For the eavesdropper, the average peak power increases by a minimum value of *4*dB and a maximum value of *9.2*dB from 16 Tx antennas, compared to the single link from either AP1 or AP2.

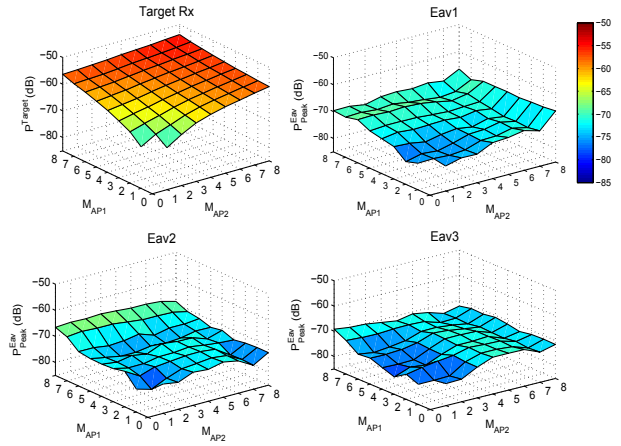


Figure 6. Average of received signal peak power with respect to the number of Tx antennas at AP1 ($M_{AP1}$) and AP2 ($M_{AP2}$), respectively.

### 4.2. Average *EM*

In this subsection, we compare the difference in received signal power between the target user and the eavesdropper, by investigating the average *EM* at $\tau=0$ and the Peak EM $EM_{\text{Peak}}$, with respect to the number of Tx antenna elements at the 2 APs.

#### *4.2.1. Average EM at τ=0*

Figure 7 shows the average *EM* as the number of Tx antenna elements varies at both AP1 and AP2. Again, due to the imbalance of the branch power and the non-coherent summation of the effective channel links at $\tau=0$, we can not observe the *3*dB increase per doubling of *M* as expected. In the single link situation (1 Tx antenna from either AP1 and AP2), a minimum average *EM* of *7*dB can be achieved over the 3 eavesdroppers. When we fully use *16* Tx antennas, the minimum *EM* for the *3* eavesdroppers is *14*dB.

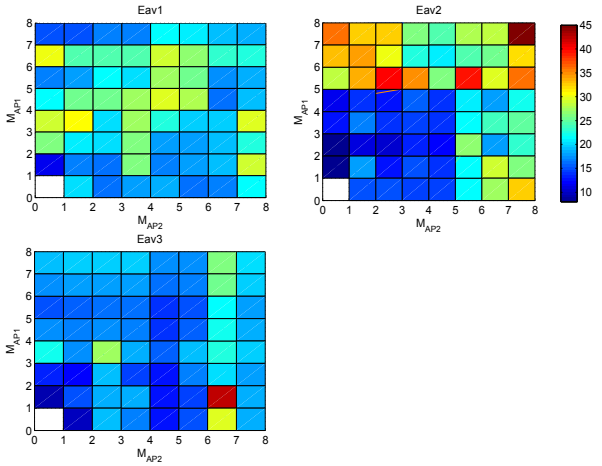


Figure 7. Average *EM* at $\tau=0$ with respect to the number of Tx antenna at AP1 ($M_{AP1}$) and AP2 ($M_{AP2}$), respectively.

This figure also indicates how we select the transmit antenna to achieve high *EM*. Let us take Eav1 as an example. In order to obtain *30*dB *EM*, we can either select *6* antenna elements from AP1, or choose *3* elements from AP1 and *1* element from AP2. A similar procedure can also be applied for Eav2 and Eav3 to achieve high *EM*. Therefore, the selection of transmit antenna can help us to reduce the

interference at each specific eavesdropper. However, in order to reduce the interference over all eavesdroppers, we need to select the transmit antennas so that we have high *EM* at all eavesdroppers.

### *4.2.2. Average Peak EM* ($EM_{Peak}$)

We also investigate the $EM_{Peak}$ in Figure 8, which indicates the lowest possible *EM*. The $EM_{Peak}$ values are smaller and fluctuate less than the average *EM*. The $EM_{Peak}$ increases as the number of transmit element increases. This trend is not clearly obvious for average *EM*. With *1* Tx element from either AP1 and AP2, the minimum $EM_{Peak}$ is *4.5*dB. With *16* Tx antennas, the minimum $EM_{Peak}$ over the *3* eavesdroppers is *13*dB.

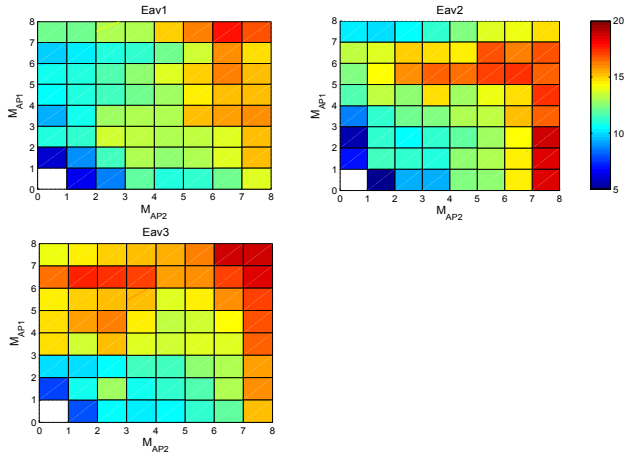


Figure 8. Average $EM_{Peak}$ with respect to the number of Tx antenna at AP1 ($M_{AP1}$) and AP2 ($M_{AP2}$), respectively.

## 8. CONCLUSIONS

This paper investigates the spatial focusing performance of MISO TR in an indoor environment with *2* distributed APs (*16* Txs) and *4* Rxs (*1* target user and *3* eavesdroppers). The feasibility of the TR application requires the Tx knows the CSI of the intended user. With the assumption of perfect channel estimation, we calculate the received signal power at $\tau=0$ and maximum power over the delay domain.

The result shows the received signal power is mainly determined by the effective channel link. In terms of unbalanced branch power, the average *EM* at $\tau=0$ and $EM_{Peak}$ are at least *7*dB and *4.5*dB for all the combinations of Tx antennas. In the presence of *16* Tx elements, the minimum average *EM* and $EM_{Peak}$ are *14*dB and *13*dB, respectively.

## 9. REFERENCES


[1] M. Fink, "Time-reversed acoustics," in *Scientific American*, pp. 91-97, Nov. 1999.

[2] M. Fink, "Time reversal of ultrasonic fields --- Part I: Basic principles," in *IEEE Trans. on Ultrasonics, Ferroelectrics and Frequency control*, vol. 39, no. 5, pp. 555-566, Sept. 1992.

[3] W.A. Kuperman, W.S. Hodgkiss, H.C. Song, T. Akal, C. Ferla, and D.R. Jackson, "Phase conjugation in the ocean: experimental demonstration of a time reversal mirror," in *J. Acoust. Soc. Am.*, vol. 103, pp. 25-40, 1998.

[4] G. Lerosey, J. de Rosny, A. Tourin, A. Derode, G. Montaldo, and M. Fink, "Time reversal of electromagnetic waves," in *Physical Review Letters*, vol. 92, no. 19, 2004.

[5] P. Kyritsi, G. Papanicolaou, and P. Stoica, "Time reversal and zero forcing for WLAN applications," in *Proceedings of the International Symposium on Wireless Personal Multimedia Coomunications (WPMC2005)*, Aalborg, Denmark. 2005.

[6] P. Kyritsi, G. Papanicolaou, P.C.F. Eggers, and A. Oprea, "MISO time reversal and delay-spread compression for FWA channels at 5GHz," in *IEEE Antennas and Wireless Propagation Letters*, vol. 3, no.6, pp. 96-99, 2004.

[7] H.T. Nguyen, J.B. Andersen, G.F. Pedersen, P. Kyritsi, and P.C.F. Eggers, "Time reversal in wireless communications: a measurement-based investigation," in IEEE Trans. on Wireless Communications, vol. 5, no. 8, pp. 2242-2252, 2006.

[8] H.T. Nguyen, J.B. Andersen, and G.F. Pedersen, "The potential use of time reversal techniques in multiple element antenna systems," in IEEE Communication Letters, vol. 9, pp. 40-42, 2005.

[9] X. Zhou, P. Kyritsi, J. M. Llorente, A. Adenet, C. Lemasson, and P.C.F. Eggers, "Assessment of MISO Time Reversal for short-range communications in the 5GHz ISM band," in Wireless Personal Communications, in press, 2007.